

Mixed state parameters of single crystalline Rb₃C₆₀ fullerene superconductors

Citation for published version (APA):

Buntar, V., Sauerzopf, M. F. M., Weber, H. W., Haluska, M., & Kuzmany, H. (2005). Mixed state parameters of single crystalline Rb₃C₆₀ fullerene superconductors. *Physical Review B: Condensed Matter*, 72(2), 024521-1/6. Article 024521. <https://doi.org/10.1103/PhysRevB.72.024521>

DOI:

[10.1103/PhysRevB.72.024521](https://doi.org/10.1103/PhysRevB.72.024521)

Document status and date:

Published: 01/01/2005

Document Version:

Publisher's PDF, also known as Version of Record (includes final page, issue and volume numbers)

Please check the document version of this publication:

- A submitted manuscript is the version of the article upon submission and before peer-review. There can be important differences between the submitted version and the official published version of record. People interested in the research are advised to contact the author for the final version of the publication, or visit the DOI to the publisher's website.
- The final author version and the galley proof are versions of the publication after peer review.
- The final published version features the final layout of the paper including the volume, issue and page numbers.

[Link to publication](#)

General rights

Copyright and moral rights for the publications made accessible in the public portal are retained by the authors and/or other copyright owners and it is a condition of accessing publications that users recognise and abide by the legal requirements associated with these rights.

- Users may download and print one copy of any publication from the public portal for the purpose of private study or research.
- You may not further distribute the material or use it for any profit-making activity or commercial gain
- You may freely distribute the URL identifying the publication in the public portal.

If the publication is distributed under the terms of Article 25fa of the Dutch Copyright Act, indicated by the "Taverne" license above, please follow below link for the End User Agreement:

www.tue.nl/taverne

Take down policy

If you believe that this document breaches copyright please contact us at:

openaccess@tue.nl

providing details and we will investigate your claim.

Mixed state parameters of single crystalline Rb_3C_{60} fullerene superconductors

V. Buntar,¹ F. M. Sauerzopf,¹ H. W. Weber,¹ M. Halushka,² and H. Kuzmany²

¹Atominstytut der Österreichischen Universitäten, Stadionallee 2, 1020 Vienna, Austria

²Institut für Materialphysik, Universität Wien, Strudlhofgasse 4, 1090 Vienna, Austria

(Received 31 October 2004; revised manuscript received 19 January 2005; published 14 July 2005)

We report on detailed magnetic investigations of big Rb_3C_{60} single crystals with sizes of ~ 1 mm. The Rb_3C_{60} crystals were prepared by doping C_{60} crystals in rubidium vapor. Experiments with different annealing times and various annealing temperatures and temperature gradients were made to assess the optimal conditions for homogeneous doping. The crystals were characterized by ac magnetization measurements. Doping at 463 K with 10% excess of rubidium and annealing at 685 K for 27 days was found to produce the best crystals with almost 100% of the pure Rb_3C_{60} phase. The temperature dependence of the upper and lower critical fields was obtained, the latter by the trapped magnetic moment method. The coherence length and the penetration depth at $T=0$ and close to the transition temperature were evaluated and the irreversibility line was determined. The results are compared to those obtained on powder and polycrystalline samples.

DOI: 10.1103/PhysRevB.72.024521

PACS number(s): 74.25.Op, 74.25.Ha, 74.25.Dw, 74.70.Wz

I. INTRODUCTION

Fullerene superconductors have attracted enormous interest of researchers for more than a decade since superconductivity in electron-doped C_{60} was discovered in 1991.¹ In the mean time, a large number of electron-doped fullerene superconductors was synthesized and thoroughly investigated (for a review see, e.g., Ref. 2). In spite of many years of the intensive research, the basic magnetic superconducting characteristics of these materials, such as the coherence length, ξ , the penetration depth, λ , the upper, H_{c2} , and the lower, H_{c1} , critical fields, are not well established for almost all of these materials, except probably for K_3C_{60} .³ Precise measurements of these properties turned out to be difficult mainly because fullerene based superconductors are extremely sensitive to air, thus preventing direct experiments requiring electrical contacts. Therefore, almost all of the results were obtained from magnetization measurements. In this type of experiment, a sample is placed into a coil in an external magnetic field and the magnetic moment measured. Because the superconductor expels external magnetic fields, the magnetic moment is diamagnetic. The field penetrates the sample on the distance of the penetration depth, λ . If the sample radius, r , is much larger than the penetration depth, the measurements will lead to correct results. In other cases, $r < \lambda$ or even $r \sim \lambda$, the experiments are difficult to interpret, because any external magnetic field will penetrate the sample almost completely, however small the field is. This implies that the sample size is a critical parameter for magnetization measurements. Previous investigations of K_3C_{60} and preliminary measurements on Rb_3C_{60} have shown that the penetration depths of these materials are of the order of $1 \mu\text{m}$.⁴ If we assume that the sample size has to be, at least, by one or two orders of magnitude larger, we end up with a minimum sample size of several tenths of a millimeter. However, almost all previous experiments were made on powders with a grain size of the order of 10 nm or on tiny crystals, which were not much larger than that. This may be the reason for the large scatter of results obtained by different groups (see Table 1 in Ref. 5).

In this paper, we report on detailed magnetic investigations of Rb_3C_{60} single crystals with volumes between 1 and 6 mm^3 , i.e., their dimensions are much larger than the penetration depth of this material. The samples were characterized by ac and dc magnetic measurements. Measurements of the main superconducting parameters, such as the critical fields and the characteristic lengths, as well as of pinning related parameters were carried out. We investigated samples of different quality with various degrees of nonsuperconducting imperfections, in order to determine the influence of these factors on the superconducting properties.

II. SAMPLE PREPARATION

The superconducting fullerides can be prepared from the corresponding molar ratio of alkali metals and C_{60} compounds, either directly from the vapor phase by two or multicomponent cosolidification,⁶ or by mixing and heating well-defined M_6C_{60} and C_{60} powders,⁷ or by doping pure C_{60} solids by the vapor of alkali metals.⁸ Sufficiently large fulleride single crystals can only be prepared by the last method. For this reason we chose the method of vapor phase doping for the preparation of Rb_3C_{60} single crystals.

C_{60} crystals with weights between 0.5 and 12 mg were selected for the doping experiments in an argon box. A few crystals with a total weight between 14 and 26 mg were placed into reaction tubes, together with a glass micropipette containing a certain amount of pure (99.6%) rubidium. Rubidium corresponding to $\sim 110\%$ of the stoichiometric amount in Rb_3C_{60} was used. The C_{60} crystals and the micropipette with rubidium were situated in the central part of the tube, which was visible through a window. The temperatures at both ends of the tube, T_{ends} , and at its central part, T_{cen} , were controlled independently. The conditions $T_{\text{ends}} > T_{\text{cen}}$ and $T_{\text{C}_{60}} > T_{\text{Rb}}$ were kept during the whole experiment.

At first the *doping* temperature was adjusted. During this stage the central part of the reaction tube with the crystals and the micropipette were at $T_{\text{cen}} = T_{\text{dop}} = 430\text{--}500$ K. When

TABLE I. Doping parameters and superconducting characteristics of three samples R3 from batch I, R28 from batch II, and R6 from batch III.

Batch (sample)	Rb/C ₆₀ ratio (%)	Doping			Annealing			T _c (K)	ΔT _c (K)
		T _{C₆₀} (K)	T _{Rb} (K)	Time (h)	T _{cry} (K)	Time (d)	Shielding fraction (%)		
I (R3)	113.8	433	433	3	685	16	137	30.7	13.6
II (R28)	110	675	495	1.7	685	11	155	30.7	6.3
III (R6)	109	463	463	1.5	685	27	115	30.9	1.3

all rubidium had evaporated from the pipette, the temperature was increased to the *annealing* temperature $T_{\text{cen}}=T_{\text{ann}}$. The crystals were kept at $T_{\text{ann}}=685$ K for ~ 0.5 –1 month. After this time the temperature was slowly decreased to room temperature.

Several batches of samples were prepared under different conditions. The variables were the stoichiometric molar ratio Rb/C₆₀, the doping temperature, the temperature gradient between Rb and C₆₀, and the annealing time. These parameters as well as the superconducting parameters of the crystals for the best three batches are shown in Table I. The first batch is represented in this work by sample R3, the second by R28, and the third by R5 and R6.

The reaction tube was then opened in an argon box. Selected crystals were inserted into 4 mm outer diameter (o.d.) quartz tubes. The crystals were fixed at the end of the tube by quartz wool. Then they were sealed at a length of about 3.5 cm. More details of the sample preparation can be found in Ref. 9.

III. SAMPLE CHARACTERIZATION

In order to obtain information about the homogeneity of the doping, magnetic measurements were performed at low temperatures. The “shielding fraction” of the sample was calculated from the value of the diamagnetic moment of the sample at low temperature. If the superconducting fraction in a sample is 100%, doping must be homogeneous, because only the Rb₃C₆₀ phase is superconducting. Due to the demagnetization factor, the apparent shielding fraction is usually larger than the superconducting fraction and can be larger than 100%. Knowing the demagnetization factor, the superconducting fraction can be calculated. From samples with 100% shielding fraction, the demagnetizing factor D was obtained experimentally from $M(H)$ and $M(T)$ zero-field-cooled (ZFC) measurements. We assume that complete flux expulsion prevails and fit the slope of the straight $M(H)$ line to $M=-H/(1-D)$, which leads to the demagnetizing factors ($D \approx 0.275$ and 0.13 for R5 and R6, respectively). For samples with $X_{\text{sh}} < 100\%$, we cannot use the experimental values and have to rely on approximate calculations.

ac measurements, which show both the real (χ') and the imaginary (χ'') part of the magnetic susceptibility, are a very powerful tool for characterizing specimens and for discriminating between intergranular and intragranular properties. With decreasing temperature the material becomes superconducting at T_c . However, the weak links are still resistive.

Therefore, in the temperature range between T_c and the temperature, where the weak links become able to carry a supercurrent, the shielding currents flow only within the grains, whereas the sample is fully shielded at lower temperatures. According to a straightforward Bean model analysis, this leads to a multiple peak structure in the χ'' dependence, in contrast to a sharp single peak for a sample without grain boundaries. At the same time, the real part of the magnetic susceptibility χ' shows the shielding of the external magnetic field.

The temperature dependence of the real and the imaginary parts of the ac susceptibility for the crystals R28, R5, and R6, and the real part for R3 are shown in Fig. 1. The sharp drop of the magnetic moment for R5 and R6 shows the transition to the superconducting state at a temperature $T_c=30.9$ K, which corresponds to that obtained from dc measurements. The width of the transition from 10% to 90% of the diamagnetic signal is about 0.9 K for R5 and 1.3 K for R6, which is very narrow and is the first evidence for a good sample quality. The peak in m'' is very sharp and close to the critical temperature. The sharpness of the peak shows that the specimen is a bulk superconductor with almost no weak links for supercurrent flow. There is still a small intergrain peak in R5, compared to the main one, which can be observed at a temperature of about 24 K. We assume that the sample is mainly a bulk crystal with some amount of small grains.

In contrast to samples R5 and R6, samples R3 and R28 exhibit a much broader transition in $m(T)$, R3 shows even two steps, which clearly indicates heavy granularity. As for R28, a complicated structure of $m''(T)$ is observed. The same sharp peak as for R5 and R6 at $T=T_c$, is also observed for R28. However, several other peaks can clearly be seen at lower temperatures. These peaks are attributed to dissipation due to weak links. Such granularity appears in the samples because of nonsuperconducting impurities (undoped C₆₀ or most probably $R \times C_{60}$) between the superconducting grains.

Summarizing the results for all three batches, the ac measurements show that all crystals from batch III are superconducting with a superconducting fraction close to 100% and no heavy granularity for current flow. The samples from batch II are very different. First, not all of them are superconducting. Those, which are superconducting, show a rather strong intergranular behavior in $m''(T)$. All crystals from batch I, although all of them are superconductors, show a two-step transition in $m(T)$ and heavy granularity in $m''(T)$.

In order to estimate the average size of the grains in samples R3, R28, R5, and R6, whose physical

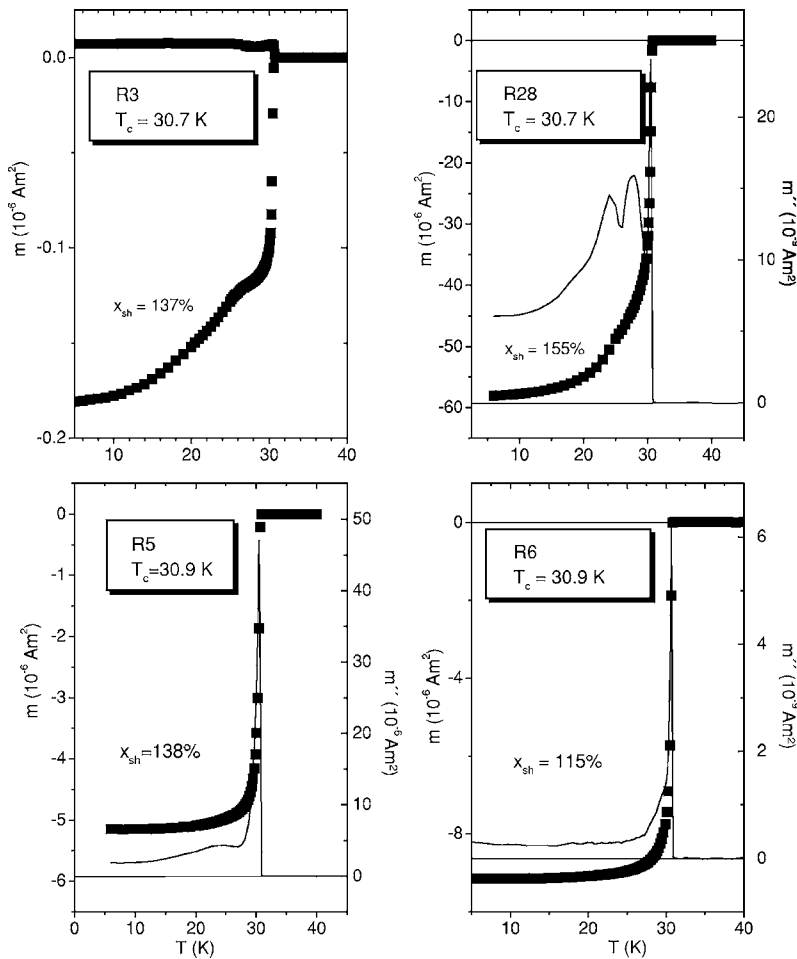


FIG. 1. Temperature dependence of the real and the imaginary part of the susceptibility obtained for R3, R28, R5, and R6 at an external magnetic field of $\mu_0 H = 0.1$ mT ($\mu_0 H = 0.5$ mT for R5). The solid symbols represent the real part of the susceptibility and the lines represent the imaginary part of the susceptibility. The shielding fraction is also indicated for each sample.

dimensions are approximately $2.6 \times 1.4 \times 1.1$ mm³, $3.3 \times 2.7 \times 1.3$ mm³, $2 \times 1.2 \times 1$ mm³, and $1.8 \times 1.5 \times 1$ mm³, respectively, we use the method suggested by Angadi *et al.*¹⁰ and later on developed for fullerene superconductors in Ref. 11. As discussed in Ref. 10, the initial slope of the magnetic moment dm/dH , along the reverse leg of a hysteresis loop right after field reversal, is a direct measure of the grain size R . This holds only over a very small field range and, therefore, requires the measurement of the magnetization in closely spaced field steps after the field reversal. For a uniform disk of radius R_s , $R_s = R$, and thickness, t , the initial slope of the reverse leg¹⁰ is given by

$$\frac{dm}{dH} = -\frac{\pi^2 R^3}{\Theta}, \quad (1)$$

where $\Theta = \ln(8 R_s/t) - 1/2$. The experimental uncertainty in the ratio R_s/t does not lead to large errors in R (for a single crystal with $R_s/t = 1$, e.g., $\Theta \sim 1.5$, and for a thin film with $R_s/t = 103$, $\Theta \sim 6.5$).

A granular sample with radius R_s contains N regions with large critical currents connected by low- J_c weak links. This can be approximated by a sample consisting of an array of N circular islands, each with radius R . The initial slope of the reverse leg for this system is given by

$$\frac{dm}{dH} = -\frac{\pi^2 R^3}{\Theta_1} = -\frac{R_s^2 R \pi^2}{\Theta_1}, \quad (2)$$

where $[\Theta_1 = \ln(8 R/t) - 1/2]$. Equation (2) is appropriate for both granular ($R < R_s$) and nongranular ($R = R_s$) samples and will be used further on.

The experimental magnetization loops on sample R6 are shown in Fig. 2, where the solid line in the insert shows the slope dm/dH . The reverse leg for R6 is smooth and wide. Similar results are found for sample R28, while R3 shows a sharp steplike return leg of the hysteresis. As shown in Ref. 11 for K_3C_{60} , the return leg of the hysteresis follows an exponential law in a sample with $R \sim R_s$, while the magnetic moment changes linearly with field in a granular sample ($R \ll R_s$) and is much steeper. These features are exactly displayed by the reverse legs found here. From Eq. (2), the corresponding radii are found to be $R \approx 500$ μm for R5, $R \approx 200$ μm for R6, $R \approx 350$ μm for R28, and $R \approx 20$ μm for R3.

From these results, we conclude that sample R3 is heavily granular even though its superconducting phase is close to or equal to 100%. The very big sample R28 has obviously several big grains of the order of several tenths of a millimeter and, most probably, extensive granular regions. The samples R5 and R6 consist of several grains, separated either by cracks or by block boundaries. The properties of these

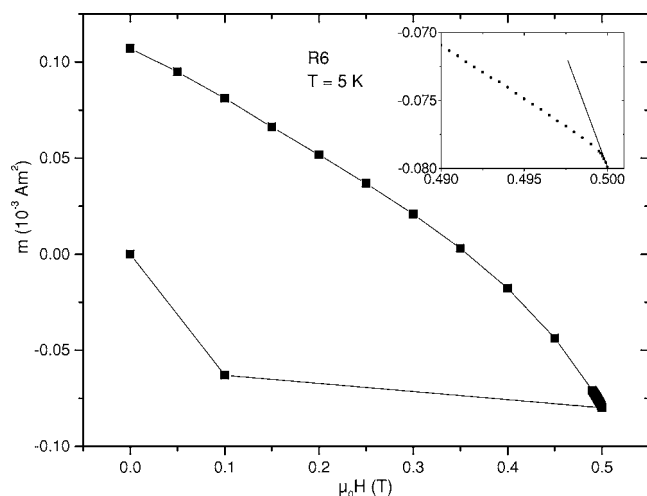


FIG. 2. Magnetization vs external magnetic field for R6 obtained at 5 K. The solid line in the insert represents the initial slope of the magnetic moment dm/dH , along the reverse leg of the hysteresis loop right after field reversal.

samples may be compared to those of melt-textured high- T_c superconductors, which also exhibit small misorientations between grains, but no granularity for the superconducting current flow. Therefore, the last two samples are considered to be suitable for the magnetic measurements of the superconducting parameters of Rb_3C_{60} .

IV. RESULTS AND DISCUSSION

A. The upper critical magnetic field

The temperature dependence of the upper critical magnetic field was obtained from field cooled (FC) curves. H_{c2} was determined in these experiments from the crossing point of extrapolations of the linear part of the magnetization $M(T)$ in the superconducting state and the small normal state magnetization neglecting fluctuation effects. It was shown on different K_3C_{60} samples,³ that the result of this experiment did not depend on the quality of a sample.

The $H_{c2}(T)$ dependence of samples R5 and R6 in fields up to 8 T is shown in Fig. 3. It is linear at these temperatures with a slope $\delta\mu_0 H_{c2}/\delta T = -4.4$ T/K, and is the same for both samples. This slope is at the upper limit of data obtained by other groups (-2 T/K $< \mu_0 H_{c2}/T < -4$ T/K, see Table 1 in Ref. 6). The extrapolation of $H_{c2}(T)$ to zero temperature is subject to considerable uncertainty and depends on the fitting scheme. To do so, the standard theory by Werthamer-Helfand-Hohenberg (WHH)¹² is usually employed (for its applicability to C_{60} -based materials, cf. Ref. 2, p. 731). The upper critical field at zero temperature $H_{c2}(0)$ can be evaluated from the relation (clean limit)

$$\mu_0 H_{c2}(0) = -0.69 T_c \frac{\delta\mu_0 H_{c2}}{\delta T}. \quad (3)$$

We obtain $H_{c2}(0) = 93$ T [as compared to 40 T $< H_{c2}(0) < 90$ T, see Table 1 in Ref. 5]. The Ginzburg-Landau relation

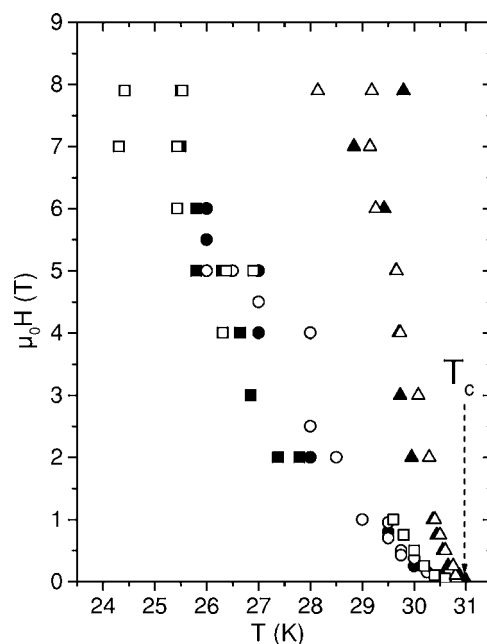


FIG. 3. Temperature dependence of the upper critical field and of the irreversibility line obtained on R5 and R6. The $H_{c2}(T)$ dependence is represented by triangles (solid for R5 and open for R6). The irreversibility line is represented by circles (R5) and squares (R6). The solid circles and squares correspond to data obtained from $M(H)$ experiments. The arrow shows the transition temperature.

$$\mu_0 H_{c2} = \frac{\Phi_0}{2\pi\xi^2}, \quad (4)$$

(where $\Phi_0 = h/2e$ is the flux quantum and ξ is the coherence length) leads to $\xi(T=0) = 1.9$ nm (compared to 2 nm $< \xi < 3$ nm, Table 1 in Ref. 5). These values are very close to those obtained by Sparn *et al.*¹³ on powder samples.

The upturn of $H_{c2}(T)$ at temperatures very close to T_c , that was observed in almost all experiments on fullerene superconductors, represents another interesting effect. As we discussed in Ref. 3, the upturn is very likely to be a consequence of the anisotropy of the Fermi surface in fullerene superconductors.¹⁴ Strong effects of the anisotropy on the magnetic properties of conventional superconductors, specifically on $H_{c2}(T)$, are well known.¹⁵

B. Irreversibility line

From the characteristic magnetic field, at which the critical current density drops below the resolution of our superconducting quantum interference device (SQUID) magnetometer, we define the irreversibility field H_{irr} . The critical current density is directly proportional to the width of the hysteresis loop ΔM . Therefore, we take as H_{irr} the field at which both positive and negative branches of an experimentally obtained hysteresis loop merge. Typical hysteresis loops are shown in Fig. 4. By measuring loops at different temperatures, the temperature dependence of the irreversibility field $H_{\text{irr}}(T)$ can be assessed. The irreversibility line obtained in this way for R5 and R6 (solid symbols) is shown in Fig. 3.

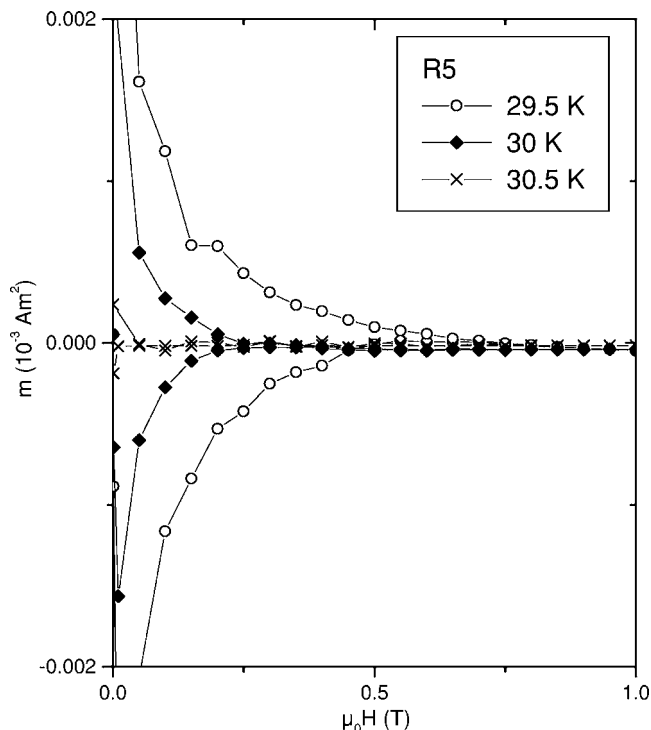


FIG. 4. Magnetization vs external magnetic field for R5 at different temperatures.

C. The lower critical magnetic field

The determination of the lower critical field by different methods, such as the first deviation from the linear $M(H)$ dependence,¹⁴ from Bean's relation $\Delta M \sim H^2$,¹⁶ from the reversible part of $M(H)$ at intermediate and high magnetic fields,¹⁷ from the measurements of irreversibility in $M(T)$ at low fields,¹⁸ etc., led to a large scatter of data. Small lower critical fields (below 5 mT) were usually attributed to breaking Josephson junctions between grains. However, the experimental results on H_{c1} were usually significantly decreasing with increasing precision of the method employed.

In order to avoid these problems, we obtained the lower critical field from measurements of the trapped magnetization, m_{tr} .³ This method is very sensitive due to the cancellation of the linear part of the magnetization. As shown for the cuprates,¹⁹ the trapped magnetization could clearly be observed at fields, where no deviation from linearity of $M(H)$ was visible. Furthermore, it is a direct measurement of the field penetrated into the sample and does not require any fitting parameters.

The experimental m_{tr} versus external magnetic field dependence obtained on R6 is shown in Fig. 5. For R6 at $T=5$ K, the trapped magnetization is close to zero up to $\mu_0 H \cong 0.6$ mT (the lower critical field at this temperature) and, at larger fields, grows proportionally to the square of the magnetic field (not shown in Fig. 5, cf. e.g., Ref. 4). This parabolic dependence confirms that the field penetrates the bulk, and not between grains.¹⁹ At $T=27$ K, m_{tr} starts to grow at significantly lower fields (see Fig. 5). The temperature dependence of H_{c1} is shown in Fig. 6. As can be seen there, no significant difference of results exists between these

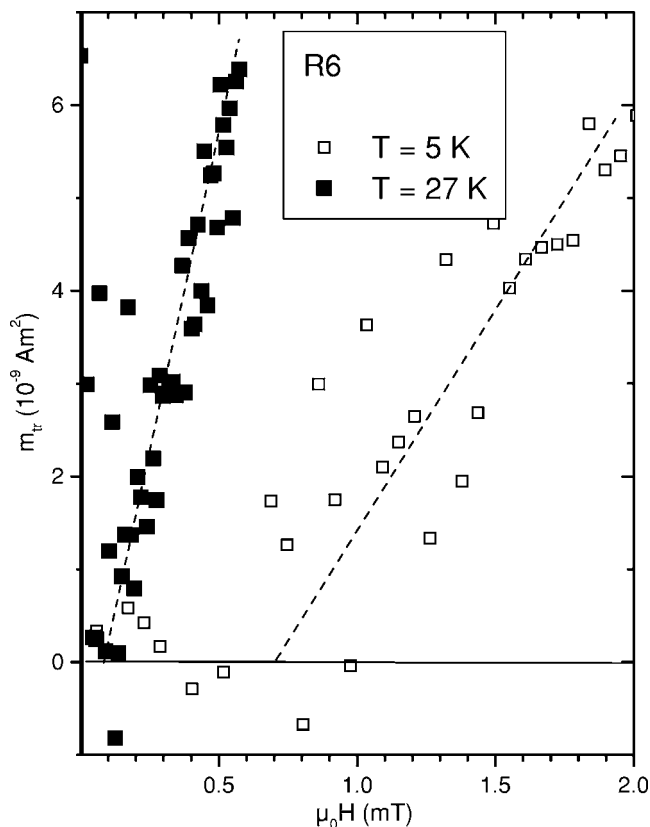


FIG. 5. Trapped magnetization vs external field for R6 at $T=5$ K (open symbols) and $T=27$ K (solid symbols). Both dashed lines are drawn to guide the eye.

two samples, i.e., the influence of the (very weak) granularity is negligible, in agreement with the results of Ref. 4.

From Fig. 6, the lower critical field at zero temperature is estimated to be $\mu_0 H_{c1}(0) = 0.91 \pm 0.2$ mT. The smallness of H_{c1} cannot be attributed to the breaking of weak links between grains because of the good sample quality and the absence of granularity, as confirmed by the ac measurements

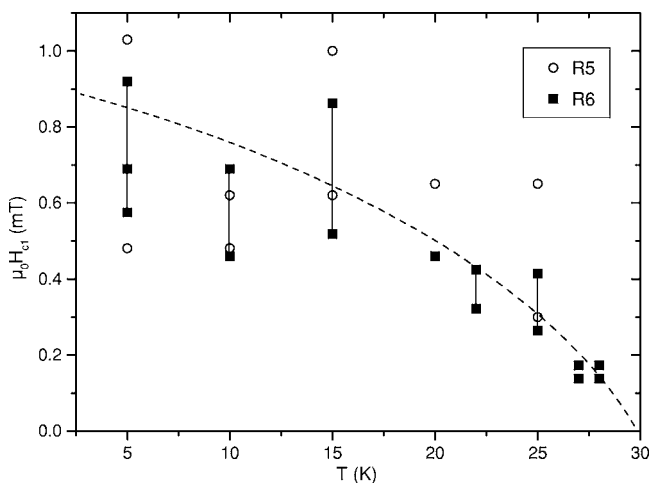


FIG. 6. Temperature dependence of the lower critical magnetic field for R5 (open symbols) and R6 (closed symbols). The dashed line is drawn to guide the eye.

and, therefore, represents an intrinsic property of this material.

The penetration depth λ at zero temperature is obtained from the equation

$$\mu_0 H_{c1} = \frac{\Phi_0}{4\pi\lambda^2} \ln \kappa. \quad (5)$$

With $\xi(0)=1.9$ nm, $\lambda(0)=1100$ nm, and, therefore, the Ginzburg-Landau parameter for Rb_3C_{60} is $\kappa=580$. This result is close to the upper limit of the data obtained by other groups ($320 < \lambda < 850$ nm). The closest is the result obtained by optical measurements.²⁰ Considering the indirect evaluation procedure to obtain λ from magnetization and μSR measurements, the difference between these results is not very large.

V. SUMMARY

In the present work, the magnetic properties of single crystalline Rb_3C_{60} fullerene superconductors with different

shielding fractions of up to 100% were investigated. ac magnetic susceptibility measurements proved the absence of granularity for the supercurrents in samples with 100% shielding fraction. An estimation of the average grain size from the slope of the reverse leg of a hysteresis loop right after field reversal, shows that some crystals did not exhibit granularity for supercurrent flow and may be considered as “true” single crystals, while others were heavily granular.

From dc magnetic measurements the upper critical field was determined and $\mu_0 H_{c2}(0)$ found to be 93 T, the slope being $\delta\mu_0 H_{c2}/\delta T = -4.4$ T/K close to T_c . No influence of the sample quality on $H_{c2}(T)$ was found. The value of the coherence length at zero temperature is $\xi=1.9$ nm.

The irreversibility line was assessed from the merging point on the hysteresis loop and found to be rather close to the upper critical field curve.

From “trapped magnetic moment” measurements the lower critical magnetic field was found to be not larger than 1 mT, the penetration depth is above 1000 nm. The Ginzburg-Landau parameter for Rb_3C_{60} is $\kappa \cong 600$.

-
- ¹A. F. Hebard, M. J. Rosseinsky, R. C. Haddon, D. W. Murphy, S. H. Glarum, T. T. M. Palstra, A. P. Ramirez, and A. R. Kortan, *Nature (London)* **350**, 600 (1991).
- ²V. Buntar, in *Fullerenes. Chemistry, Physics, and Technology*, edited by K. M. Kadish and R. S. Ruoff (Wiley, New York, 2000).
- ³V. Buntar, F. M. Sauerzopf, H. W. Weber, J. E. Fischer, H. Kuzmany, and M. Haluska, *Phys. Rev. B* **56**, 14 128 (1997).
- ⁴V. Buntar, F. M. Sauerzopf, and H. W. Weber, *Phys. Rev. B* **54**, R9651 (1996).
- ⁵V. Buntar and H. W. Weber, *Supercond. Sci. Technol.* **9**, 599 (1996).
- ⁶Y. Iwasa, K. Tanaka, T. Yasuda, and T. Koda, *Phys. Rev. Lett.* **69**, 2284 (1992).
- ⁷J. P. McCauley, Jr., Q. Zhu, N. Coustel, O. Zhou, G. Vaughan, S. H. Idziak, J. E. Fisher, S. W. Tozer, D. M. Groski, N. Bykovetz, C. L. Lin, A. R. McGhie, B. H. Allen, W. J. Romanow, A. M. Denenstein, and A. B. Smith III, *J. Am. Chem. Soc.* **113**, 8537 (1991).
- ⁸M. Haluska, V. Buntar, C. Krutzler, and H. Kuzmany, in *Recent Advances in the Chemistry and Physics of Fullerenes and Related Materials*, edited by M. Kadish, R. S. Ruoff (1998), p. 436.
- ⁹V. Buntar, M. Haluska, H. Kuzmany, F. M. Sauerzopf, and H. W. Weber, *Supercond. Sci. Technol.* **16**, 907 (2003).
- ¹⁰M. A. Angadi, A. D. Caplin, J. R. Lavery, and Z. X. Shen, *Physica C* **177**, 479 (1991).
- ¹¹V. Buntar, F. M. Sauerzopf, C. Krutzler, and H. W. Weber, *Phys. Rev. Lett.* **81**, 3749 (1998).
- ¹²N. R. Werthamer, E. Helfand, and P. C. Hohenberg, *Phys. Rev.* **147**, 295 (1966).
- ¹³M. Lopez-Cabrera, D. Z. Goodson, D. R. Herschbach, and J. D. Morgan III, *Phys. Rev. Lett.* **68**, 1228 (1992).
- ¹⁴S. C. Erwin and W. E. Pickett, *Science* **254**, 842 (1991).
- ¹⁵*Anisotropy Effects in Superconductors*, edited by H. W. Weber (Plenum Press, New York, 1977).
- ¹⁶V. Buntar, U. Eckern, and C. Politis, *Mod. Phys. Lett. B* **6**, 1037 (1992).
- ¹⁷V. Buntar, M. Ricco, L. Cristofolini, H. W. Weber, and F. Bolzoni, *Phys. Rev. B* **52**, 4432 (1995).
- ¹⁸M. Kraus, H. Sindlinger, H. Werner, R. Schlögl, V. Thommen, H. P. Lang, H.-J. Gütherodt, and K. Lüders, *J. Phys. Chem. Solids* **57**, 999 (1996).
- ¹⁹V. Moshchalkov, J. V. Henry, C. Marin, J. Rossat-Mignod, and J. F. Jacquot, *Physica C* **175**, 407 (1991).
- ²⁰L. Degiorgi *et al.*, *Phys. Rev. Lett.* **69**, 2987 (1992).